Mutations of the Sonic Hedgehog Pathway Underlie Hypothalamic Hamartoma with Gelastic Epilepsy

Michael S. Hildebrand,[1,13] Nicole G. Griffin,[2,13] John A. Damiano,[1] Elisa J. Cops,[1] Rosemary Burgess,[1] Ezgi Ozturk,[3] Nigel C. Jones,[3] Richard J. Leventer,[4,5,6] Jeremy L. Freeman,[4] A. Simon Harvey,[4,5,6] Lynette G. Sadleir,[7] Ingrid E. Scheffer,[1,5,8] Heather Major,[9] Benjamin W. Darbro,[9] Andrew S. Allen,[10] David B. Goldstein,[2] John F. Kerrigan,[11] Samuel F. Berkovic,[1,13,*] and Erin L. Heinzen[2,12,13,*]

Hypothalamic hamartoma (HH) with gelastic epilepsy is a well-recognized drug-resistant epilepsy syndrome of early life.[1] Surgical resection allows limited access to the small deep-seated lesions that cause the disease. Here, we report the results of a search for somatic mutations in paired hamartoma- and leukocyte-derived DNA samples from 38 individuals which we conducted by using whole-exome sequencing (WES), chromosomal microarray (CMA), and targeted resequencing (TRS) of candidate genes. Somatic mutations were identified in genes involving regulation of the sonic hedgehog (Shh) pathway in 14/38 individuals (37%). Three individuals had somatic mutations in *PRKACA*, which encodes a cAMP-dependent protein kinase that acts as a repressor protein in the Shh pathway, and four subjects had somatic mutations in *GLI3*, an Shh pathway gene associated with HH. In seven other individuals, we identified two recurrent and three single brain-tissue-specific, large copy-number or loss-of-heterozygosity (LOH) variants involving multiple Shh genes, as well as other genes without an obvious biological link to the Shh pathway. The Shh pathway genes in these large somatic lesions include the ligand itself (*SHH* and *IHH*), the receptor *SMO*, and several other Shh downstream pathway members, including *CREBBP* and *GLI2*. Taken together, our data implicate perturbation of the Shh pathway in at least 37% of individuals with the HH epilepsy syndrome, consistent with the concept of a developmental pathway brain disease.

Some brain malformation syndromes are due to inherited germline mutations or germline or post-zygotic de novo mutations (reviewed in Poduri et al.[2]). Yet the cause of most brain malformations, with their frequent consequences of refractory epilepsy and intellectual disability, remains unknown. Recently, exome sequencing studies in privileged situations in which brain tissue is available have highlighted the role of somatic mutations confined to the brain. For example, somatic mutations in mTOR pathway genes (e.g., *PIK3CA* [MIM: 171834], *AKT3* [MIM: 611223], and *MTOR* [MIM: 601231]) have been found to be important for a variety of malformations of cortical development, ranging from large hemispheric malformations to small focal cortical dysplasias.[3–6] Outside these rare disorders, the role of somatic mutations in drug-resistant epilepsies is largely unexplored.[7,8] Because the very rare dominant disorder of Pallister-Hall syndrome (MIM: 146510), comprising hypothalamic hamartomas (HHs [MIM: 241800]) and various other congenital anomalies, is due to germline truncation mutations in *GLI3* (MIM: 165240),[9] we previously searched for somatic *GLI3* mutations in hamartoma tissue. We established that a few cases have de novo somatic point mutations or copy-number variants (CNVs) at this locus,[10,11] a finding that has now been independently confirmed.[12] These early observations motivated a genome-wide search for somatic mutations via our unique access to hamartoma tissue and venous blood from individuals with HH. Surgical removal of these lesions was once regarded as hazardous. The development of innovative surgical techniques[13] led to a relatively large series of this rare disorder being available at The Royal Children's Hospital and The Barrow Institute.

Herein, we studied DNA extracted according to standard protocols from freshly frozen or formalin-fixed paraffin-embedded hamartoma tissue and leukocytes of 38 individuals with HH to identify somatic mutations. The human research ethics committees of the Austin Hospital and The Royal Children's Hospital in Melbourne and the institutional review board of St. Joseph's Hospital and Medical Center in Phoenix approved this study. Informed consent was obtained from affected individuals or their parents or legal guardians in the case of minors, those with intellectual disability, or deceased individuals. There were 11 females and 27 males, all with intractable epilepsy (Table S1). Epilepsy began in the first year of life in 30/38 of these indivdiuals, and all had gelastic (laughing) seizures.

[1]Epilepsy Research Center, Department of Medicine, The University of Melbourne and Austin Health, Heidelberg, VIC 3084, Australia; [2]Institute for Genomic Medicine, Columbia University, New York, NY 10032, USA; [3]Department of Medicine, The University of Melbourne and The Royal Melbourne Hospital, Parkville, VIC 3050, Australia; [4]Department of Neurology, The Royal Children's Hospital, Parkville, VIC 3052, Australia; [5]Department of Paediatrics, University of Melbourne and The Royal Children's Hospital, Parkville, VIC 3052, Australia; [6]Murdoch Childrens Research Institute, The Royal Children's Hospital, Parkville, VIC 3052, Australia; [7]Department of Paediatrics and Child Health, University of Otago, Wellington 9016, New Zealand; [8]The Florey Institute of Neuroscience and Mental Health, Parkville, VIC 3052, Australia; [9]Department of Pediatrics, The University of Iowa, Iowa City, IA 52246, USA; [10]Department of Biostatistics and Bioinformatics, Duke University, Durham, NC 27710, USA; [11]Division of Pediatric Neurology, Barrow Neurological Institute, Phoenix Children's Hospital, Phoenix, AZ 85013, USA; [12]Department of Pathology and Cell Biology, Columbia University, New York, NY 10032, USA
[13]These authors contributed equally to this work
*Correspondence: s.berkovic@unimelb.edu.au (S.F.B.), eh2682@cumc.columbia.edu (E.L.H.)
http://dx.doi.org/10.1016/j.ajhg.2016.05.031.

Additional features included intellectual disability in 24 individuals and central precocious puberty in 14 individuals; however, none had additional syndromic features of digital, oro-facial abnormalities or visceral malformations and none had a family history of HH. Samples were subjected to whole-exome sequencing (WES) as described previously[14,15], chromosomal microarray (CMA; Figure S1), and targeted resequencing (TRS) of 50 genes in the Shh pathway (Roche SeqCap EZ); the methodology selected depended on the quality and quantity of DNA from the brain samples. Due to limited DNA, nine hamartoma DNA samples were whole-genome amplified (QIAGEN Repli-g Single Cell) prior to WES.

Our first experiment was to subject a subset of paired DNA samples from hamartomas and leukocytes to WES (n = 15). Somatic single-nucleotide variants (sSNVs) were called from the aligned BAM files in both VarScan-2 and Mutect.[16] VarScan-2 was used to call somatic insertion-deletion variants (sindels).[17] sSNVs were removed from consideration if they were called in regions where there was less than 10-fold sequencing coverage in either the hamartoma or leukocytes, if the variant was present in less than three sequencing reads in the hamartoma, and if the variant was present in more than 5% of reads from leukocytes. Sindels with strand bias were filtered out with the Phred-scaled strand bias score. A somatic variant was classified as a candidate variant if it was predicted to change or truncate the amino acid sequence (Ensembl Variant Effect Predictor); this included missense (possibly- or probably-damaging or unknown according to PolyPhen-2), nonsense (frameshift and stop), and splice-site variants that were not present in controls sequenced in house (Institute for Genomic Medicine), in the Exome Variant Server (EVS), or in the Exome Aggregation Consortium (ExAC) database. The number of sSNVs and sindels detected in surgically resected tissue from the individuals with HH varied, despite high average coverage across exons (~100 fold; Table S2). A total of 374 sSNVs were called on average per sample, including 12 candidate variants on average per sample (Tables S2 and S3). An average of 254 sindels were detected per sample, of which four on average per sample were candidate variants (Tables S2 and S3). Not unexpectedly, the nine samples for which the hamartoma DNA was whole-genome amplified due to very limited amounts of starting material prior to the preparation of the sequencing library produced larger numbers of sSNVs and sindels, most likely due to amplification artifacts. Among unamplified samples, 175 ± 51 and 186 ± 36 sSNVs and sindels, respectively, were called, versus 507 ± 479 sSNVs and 300 ± 211 sindels in the amplified samples (Table S2).

We performed a pathway analysis to determine whether candidate variants detected through WES were statistically significantly enriched in the Shh signaling pathway or any other Kyoto Encyclopedia of Genes and Genomes (KEGG) pathways (n = 301)[18] by comparing the observed per base rate of candidate variants within and outside the pathway for each individual to the null expectation, estimated from the total number of candidate variants observed in the exome, the relative proportion of exonic bases within and outside the pathway that were sufficiently sequenced in the hamartoma and leukocyte DNA to call a candidate variant, and the relative mutability of the sequences within and outside of the pathway (see Supplemental Note). Two pathways of the 301 tested were enriched for candidate variants: the Shh pathway ($p = 3 \times 10^{-5}$) and the salivary secretion pathway ($p = 0.017$).

We next evaluated whether any genes in these two pathways were significantly enriched for candidate variants. *GLI3* and *PRKACA* ([MIM: 601639], see Supplemental Note), both of which are involved in the Shh signaling pathway (defined by KEGG), were found to have two and three candidate variants, respectively, all in different individuals (Table 1). The uncorrected p values of seeing two and three candidate variants in *GLI3* and *PRKACA* were 0.0025 and 2×10^{-7}, respectively. Correcting for the ~18,000 protein-coding genes genome wide, *PRKACA* is significantly enriched for candidate variants, implicating *PRKACA* as a HH-associated gene. We note that *PRKACA* encodes a protein that is named in both the Shh signaling and salivary secretion pathways (defined by KEGG). Given the existing evidence for the Shh signaling pathway in HH pathophysiology,[10–12] we believe somatic variants in *PRKACA* lead to HH through disruption of the Shh signaling pathway. In addition to *PRKACA*, one additional gene, *ZNF362*, harboring a recurrent somatic mutation found in three individuals (Table S3), was found to be significantly enriched genome wide for candidate variants. These variants were found to be selectively observed in DNA specimens that were exome sequenced after whole-genome amplification in this study and in DNA from 12 out of 20 other individuals (without HH) that were also sequenced after whole-genome amplification as part of other genetic studies and therefore were not pursued further.

To screen for additional somatic mutations in *PRKACA* and *GLI3,* we then performed Sanger sequencing of the protein-coding exons by using standard protocols in hamartoma and blood DNA of 20 individuals with HH from our cohort that had not already been subjected to WES and identified a frameshift indel in *PRKACA* in an additional individual (hht25085; Table 1).

In addition to sSNVs and sindels, two large somatic loss-of-heterozygosity (sLOH) events were observed in the 15 samples analyzed by exome sequencing (Figure S2). One individual had sLOH across the p arm of chromosome 16, and another had sLOH across the q arm of chromosome 7 (Table 1; Figure 1). Interestingly, both regions contain genes connected to the Shh pathway; both *SHH* (MIM: 600725) and *SMO* (MIM: 601500), as well as *WNT16* (MIM: 606267) and *WNT2* (MIM: 147870), are located in the sLOH region on the q arm of chromosome 7; a transcriptional co-activator of the pathway, *CREBBP* (MIM: 600140), is located in the sLOH region on chromosome 16p.

Table 1. Study Participants with Confirmed Somatic Mutations in or Linked to the Shh Pathway

Subject	Genomic Analysis Method(s)			Annotation of Candidate Mutations	Shh Gene(s) (KEGG)	VAF Brain	VAF Blood	Method of Detection
	WES	CMA	TRS					
hht25086	×	–	–	c.984dupT (p.Asp329Ter) [GenBank: NM_002730.3]	*PRKACA*	25%	0.5%	WES, confirmed by Sanger
hht238a	×	–	–	c.983_984delTT (p.Phe328Ter) [GenBank: NM_002730.3]	*PRKACA*	23%	0%	WES, confirmed by Sanger
hht1198c	×	×	–	chr7q LOH (chr7:58,814,064–159,138,663)	*SHH, SMO, WNT16, WNT2*	NA	NA	WES, confirmed by CMA
hht735	×	×	×	chr16p LOH (chr16:0–31,543,619)	*CREBBP*[a]	NA	NA	WES, confirmed by CMA
hht209	×	–	–	c.2989dupG (p.Ala997GlyfsTer87) [GenBank: NM_000168.5]	*GLI3*	57%	0%	WES, confirmed by Sanger
hht26139	×	–	–	c.3442C>T (p.Gln1148Ter) [GenBank: NM_000168.5]	*GLI3*	24%	0%	WES, confirmed by Sanger
hht880	–	×	–	chr2q12.1–q37.3 LOH (chr2:103,856,408–243,199,373)	*GLI2, IHH, LRP2, STK36, WNT10A, WNT6*	NA	NA	CMA
hht953	–	×	–	chr14q11.2–q32.33 LOH (chr14:24,419,118–106,072,470)	*BMP4, AKT1*	NA	NA	CMA
hht25057	–	×	–	chr16p11.2–p13.3 LOH (chr16:0–31543619)	*CREBBP*[a]	NA	NA	CMA
hht25063	–	×	–	chr7p22.1–q36.3 CNG, CNL (chr7:986211–60069242, 58814064–159138663)	*GLI3, SHH, SMO, WNT16, WNT2*	NA	NA	CMA
hht25094	–	×	–	chr11q12.3–q25 LOH (chr11:64879188–135006516)	*WNT11*	NA	NA	CMA
hht25077	–	×	×	c.3172C>T (p.Arg1058Ter) [GenBank: NM_000168.5]	*GLI3*	18%	0%	TRS, confirmed by Sanger
hht31536	–	×	×	c.2071C>T (p.Gln691Ter) [GenBank: NM_000168.5]	*GLI3*	37%	0.8%	TRS, confirmed by Sanger
hht25085	–	–	–	c.226-231dup (p.Asp76_Lys77dup) [GenBank: NM_002730.3]	*PRKACA*[b]	–	–	Sanger

Shh, sonic hedgehog; VAF, variant allele frequency; LOH, loss of heterozygosity (might be copy-number neutral LOH); CNG, copy-number gain; CNL, copy-number loss; WES, whole-exome sequencing; CMA, chromosomal microarray; TRS, targeted resequencing; ×, used; –, not used; NA, not applicable. All coordinates correspond to the UCSC Genome Browser reference genome (GRCH37/hg19).
[a]Transcriptional regulator of the Shh pathway.
[b]Identified by Sanger sequencing.

Because four of the five candidate variants were putatively protein-truncating mutations and because we observed two large LOH events with WES, we then used CMA to screen for somatic genomic deletions and other CNVs genome wide in 28 HH cases with adequate tumor DNA. We included the two exome-sequenced samples harboring large LOH regions on chromosomes 7q or 16p to confirm the detected somatic events. Analysis revealed a large somatic event in seven of the 28 individuals with HH, including confirmation of the two LOH lesions found by WES (Table 1; Figures S1 and S2). The lesions at 7q and 16p deletions were recurrent, given that one additional individual was found with copy-number neutral LOH (CNNLOH) events at each of these loci (Table 1). Three non-recurrent CNV or LOH events were also identified. One was found on chromosome 2q and included the Shh and/or WNT pathway members *IHH* (MIM: 600726), *STK36* (MIM: 607652), *GLI2* (MIM: 165230), *LRP2* (MIM: 600073), *WNT10A* (MIM: 606268), and *WNT6* (MIM: 604663). The second was on chromosome 14q and encompassed *BMP4* (MIM: 112262) and *AKT1* (MIM: 164730), a gene encoding a protein known to interact with the Shh pathway[19] and that, when mutated, can result in a common type of primary brain tumor (meningioma).[20] A third was discovered on chromosome 11q and included the Shh and/or WNT pathway members *WNT11* (MIM: 603699) and *LRP5* (MIM: 603506). The WNT pathway has parallel roles during development to the Shh signaling pathway[21] and is also critical for axon guidance.[22] A simulation analysis to assess the probability of observing this number of Shh genes in randomly selected (see Supplemental Note), similarly sized CNV or LOH events throughout the genome was significant ($p = 0.046$). We also performed a simulation analysis for the salivary secretion pathway but did not observe a significant enrichment for genes in this pathway ($p = 0.716$).

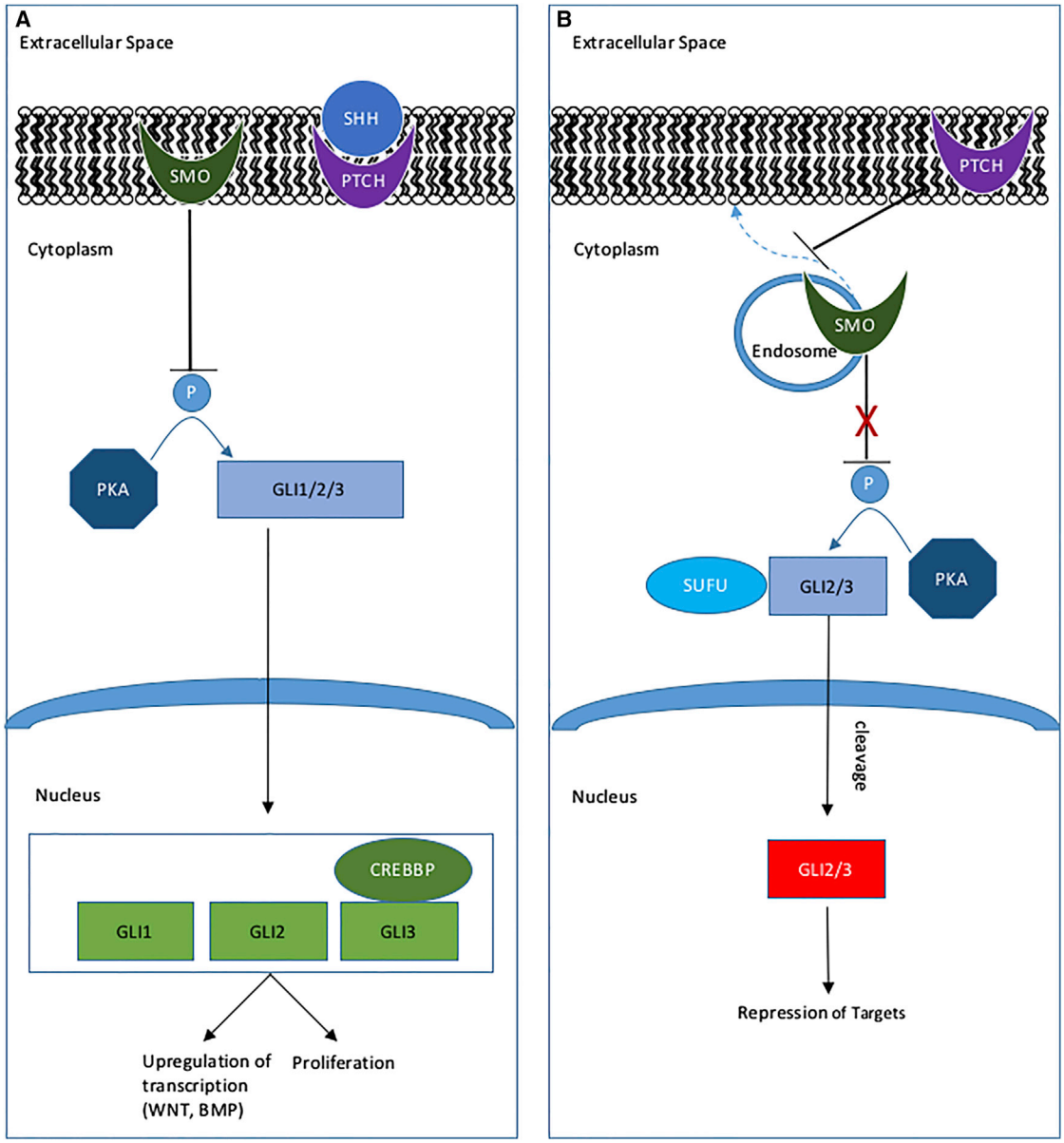

Figure 1. Shh Pathway Showing Some of the Proteins Implicated in HH

(A) In the presence of SHH, PTCH no longer inhibits SMO from translocating to the membrane, where it inhibits phosphorylation of GLI2 and GLI3 by PKA (*PRKACA*). Full-length GLI2 and GLI3 translocate to the nucleus and, together with GLI1 and the transcriptional coactivator CREBBP, promote transcription of downstream target genes[9]

(B) In the absence of SHH, SMO remains localized to endosomes in the cytoplasm. GLI2 and GLI3 are bound by the SUFU complex and phosphorylated by PKA,[15] leading to their cleavage. The cleaved protein translocates to the nucleus, where it acts to repress target gene transcription.

14 out of 38 individuals with HH had confirmed somatic mutations in the Shh pathway; an additional five individuals had unconfirmed findings in this pathway. Four individuals had confirmed somatic point mutations in *GLI3*, and an additional individual had a CNV that encompassed this gene. Three individuals had confirmed somatic mutations in *PRKACA*. Other proteins in the Shh pathway implicated in HH because of their occurrence in CNVs are SHH, SMO, CREBBP, GLI2, and STK36 (or, FU). Not shown on this simplified diagram are *IHH*, *LRP2*, *LRP5*, *AKT1*, and specific WNT and BMP pathway members that encode proteins in the Shh pathway, or that closely interact with the pathway, and are located within CNVs found in individuals with HH.[16–19]

Given the preponderance of candidate somatic mutations in Shh genes, we then performed TRS of 50 genes in the Shh signaling pathway, as defined by KEGG,[18] as well as of the transcriptional coactivator, *CREBBP*, in 15 individuals with HH to further screen for candidate causal mutations (see Supplemental Note for further methodological details). This analysis revealed somatic mutations in two additional individuals, both nonsense mutations in *GLI3*, confirmed by Sanger sequencing (Table 1). It is noteworthy that two of eight mutations in *GLI3* and *PRKACA* detected by WES or TRS were present in a small fraction of sequencing reads from leukocyte-derived DNA,

Table 2. Study Participants with No Candidate or Unconfirmed Candidate Somatic Mutations in or Linked to the Shh Pathway

Subject	Genomic Analysis Method(s)			Annotation of Candidate Mutations	Shh Gene(s) (KEGG)	VAF Brain	VAF Blood	Method of Detection
	WES	CMA	TRS					
hht929	×	×	×	c.494dupG (p.Cys168LeufsTer4) [GenBank: NM_057168.1]	*WNT16*[a]	31%	4%	WES, TRS
hht25093 g	×	–	–	c.248T>C (p.Leu83Pro) [GenBank: NM_002730.3]	*PRKACA*	14%	1%	WES
hht20138	–	×	×	c.984dupT (p.Asp329Ter) [GenBank: NM_002730.3]	*PRKACA*	25%	0%	TRS
hht25060	–	×	×	c.1025dupG (p.Ala343ArgfsTer35) [GenBank: NM_003393.3]	*WNT8B*	28%	0%	TRS
				c.394C>T (p.Gln132Ter) [GenBank: NM_182948.2]	*PRKACB*	25%	0%	
				c.5293dupC (p.Gln1765ProfsTer201) [GenBank: NM_004380.2]	*CREBBP*[b]	14%	0%	
hht25186	–	–	×	c.6858dupT (p.Glu2287Ter) [GenBank: NM_004525.2]	*LRP2*	17%	3%	TRS
				c.4230dupT (p.Gly1411TrpfsTer10) [GenBank: NM_004380.2]	*CREBBP*[b]	14%	0%	
hht25064	–	–	×	ND	NA	NA	NA	
hht1276d	×	–	–	ND	NA	NA	NA	
hht322b	×	×	–	ND	NA	NA	NA	
hht25132h	×	×	–	ND	NA	NA	NA	
hht786	×	×	×	ND	NA	NA	NA	
hht25080	×	×	×	ND	NA	NA	NA	
hht25099	×	×	×	ND	NA	NA	NA	
hht25059	–	×	×	ND	NA	NA	NA	
hht25082	×	–	×	ND	NA	NA	NA	
hht25050	–	×	–	ND	NA	NA	NA	
hht25054	–	×	–	ND	NA	NA	NA	
hht25066	–	×	–	ND	NA	NA	NA	
hht25072	–	×	–	ND	NA	NA	NA	
hht25079	–	×	–	ND	NA	NA	NA	
hht25089	–	×	–	ND	NA	NA	NA	
hht25097	–	×	–	ND	NA	NA	NA	
hht25098	–	×	–	ND	NA	NA	NA	
hht25052	–	×	×	ND	NA	NA	NA	
hht25056	–	×	×	ND	NA	NA	NA	

Shh, Sonic hedgehog; VAF, variant allele frequency; WES, whole-exome sequencing; CMA, chromosomal microarray; TRS, targeted resequencing; ×, used; –, not used; NA, not applicable; ND, none detected. All coordinates correspond to the UCSC Genome Browser reference genome (GRCH37/hg19).
[a]Candidate mutation found in *WNT16* was detected with both next-generation sequencing technologies but not confirmed with Sanger sequencing because of insufficient DNA.
[b]Transcriptional regulator of the Shh pathway.

albeit a much smaller fraction than in tumors, and not confirmed to be present with another genotyping method (Table 1). This suggests that the mutations might be diffusely expressed in the brain, rather than just in the hamartoma per se. This is consistent with the observation of germline mutations in *GLI3* in Pallister-Hall syndrome, in which HH is usually the only lesion in the brain.[9] Although the biological significance of the observed enrichment of candidate variants in the salivary secretion pathway genes in HH is unclear, we did not further pursue these variants given that we detected no enrichment of genes in this pathway in somatic CNVs. Additionally, we note that Saitsu et al., who also recently screened for somatic mutations in HH, further support the association of the Shh pathway

with HH with their work and did not report somatic mutations in the salivary secretion pathway genes.[12]

We predict that the somatic mutations in the pathway could lead to reduced Shh signaling. GLI3 can act as both a transcriptional activator and repressor of downstream targets.[23] In the absence of Shh, protein kinase A (PKA) phosphorylates GLI3, causing its cleavage into a repressor form of the protein (Figure 1[23]). This repressor then translocates to the nucleus and suppresses transcription of target genes. The somatic mutations we discovered in *GLI3* all occurred in the same region as germline mutations in Pallister-Hall syndrome. The mutant, truncated protein in Pallister-Hall syndrome has been shown to localize to the nucleus and repress expression of target genes, leading to less Shh signaling.[24] Two of three confirmed *PRKACA* mutations were located in the C-terminal region of the catalytic subunit; these truncating mutations could impair binding of the regulatory subunit of PKA, leading to a constitutively active form of the protein and subsequent repression of target genes due to increased phosphorylation and cleavage of GLI3. Interestingly, in adrenocortical tumors, a recurrent somatic mutation (encoding p.Leu206Arg) in *PRKACA* has been shown to inhibit binding of the regulatory subunit of PKA, leading to constitutive activation of the catalytic subunit of PKA and increased phosphorylation activity.[25,26]

In summary, this comprehensive analysis revealed 14 somatic mutations (four nonsense changes, two frameshift indels, one in-frame insertion, and seven large CNV or LOH events; Table 1; Figure 1) in Shh pathway genes. *PRKACA* is now securely implicated as a HH-associated gene, in addition to the previously associated Shh gene, *GLI3*.[10–12] An additional fifteen genes (*AKT1*, *BMP4*, *CREBBP*, *GLI2*, *IHH*, *LRP2*, *LRP5*, *SHH*, *SMO*, *STK36*, *WNT2*, *WNT6*, *WNT10A*, *WNT11*, and *WNT16*) associated with the Shh tumor suppressor pathway and the related WNT pathway are potentially implicated, as well as, possibly, other genes (within the large CNV or LOH regions) that do not have an obvious biological link to the Shh pathway. We did not identify somatic mutations in *OFD1* (MIM: 300170), a recently reported candidate HH-associated gene identified in a mix of sporadic and syndromic cases from the Japanese population.[12] Five cases had "unconfirmed findings" because there was insufficient DNA to complete the validation of all variants detected, whereas for 19 cases, no variants in genes encoding proteins directly or indirectly related to Shh were discovered (Table 2). Thus, we identified potentially pathogenic mutations in the Shh pathway in at least 37% (14/38) of individuals with HH, and possibly as many as 50% (19/38). This aggregation to a particular pathway is reminiscent of the remarkable contribution of various mTOR pathway gene mutations to malformations of cortical development, realized through similar clinico-molecular studies with privileged brain tissue over the last few years.[2,3,27] The intense interest in Shh signaling in a variety of cancers has led to the development of potentially therapeutic agents acting on this pathway that could also be explored in treating this syndrome.[28,29]

Supplemental Data

Supplemental Data include a Supplemental Note, two figures, three tables, and supplemental acknowledgments and can be found with this article online at http://dx.doi.org/10.1016/j.ajhg.2016.05.031.

Conflicts of Interest

I.E.S. discloses payments from UCB Pharma and Athena Diagnostics and Transgenomics for lectures and educational presentations. D.B.G. is an equity holder in Pairnomix, a company focused on modeling epilepsy mutations. S.F.B. discloses payments from UCB Pharma, Novartis Pharmaceuticals, Sanofi-Aventis, and Janssen Cilag for lectures and educational presentations and a patent for SCN1A testing held by Bionomics Inc. and licensed to various diagnostic companies.

Acknowledgments

We thank the families for their participation in this study, and we value the advocacy from the Hope for Hypothalamic Hamartoma Foundation (http://hopeforhh.org). Elena Aleksoska (Epilepsy Research Centre) performed genomic DNA extractions from tissues. Brett Copeland, Joshua Bridgers, and Sitharthan Kamalakaran (Institute for Genomic Medicine) provided bioinformatics support. Dr. Paul Lockhart, Greta Gillies, and Kate Pope (Murdoch Childrens Research Institute) assisted with collection of tissue, and Jeffrey Rosenfeld and Wirginia Maixner (Royal Children's Hospital, Melbourne) performed surgeries. This study was supported by a National Health and Medical Research Council (NHMRC) Program Grant (628952) to S.F.B. and I.E.S., a Practitioner Fellowship (1006110) to I.E.S, and a Career Development Fellowship (1063799) to M.S.H. I.E.S. was also funded by grants from the NIH, Australian Research Council, Health Research Council of New Zealand, CURE, American Epilepsy Society, US Department of Defense Autism Spectrum Disorder Research Program, March of Dimes, and Perpetual Charitable Trustees. E.L.H. was supported by a NIH grant (R21-NS078657). N.C.J. was supported by an Australian Research Council Future Fellowship (13100100). Acknowledgments of individuals and funding sources responsible for the samples used in this study as controls are provided in the Supplemental Data.

Received: February 3, 2016
Accepted: May 26, 2016
Published: July 21, 2016

Web Resources

Consensus Coding Sequence, https://www.ncbi.nlm.nih.gov/CCDS/
ExAC Browser, http://exac.broadinstitute.org/
GenBank, http://www.ncbi.nlm.nih.gov/genbank/
Ingenuity Pathway Analysis, http://www.qiagen.com/ingenuity
Kyoto Encyclopedia of Genes and Genomes, http://www.genome.jp/kegg/
NCBI Gene, http://www.ncbi.nlm.nih.gov/gene

NHLBI Exome Sequencing Project (ESP) Exome Variant Server, http://evs.gs.washington.edu/EVS/
OMIM, http://www.omim.org/
UCSC Genome Browser, http://genome.ucsc.edu
Variant Effect Predictor, http://useast.ensembl.org/Homo_sapiens/Tools/VEP

References

1. Berkovic, S.F., Arzimanoglou, A., Kuzniecky, R., Harvey, A.S., Palmini, A., and Andermann, F. (2003). Hypothalamic hamartoma and seizures: a treatable epileptic encephalopathy. Epilepsia *44*, 969–973.
2. Poduri, A., Evrony, G.D., Cai, X., and Walsh, C.A. (2013). Somatic mutation, genomic variation, and neurological disease. Science *341*, 1237758.
3. Lee, J.H., Huynh, M., Silhavy, J.L., Kim, S., Dixon-Salazar, T., Heiberg, A., Scott, E., Bafna, V., Hill, K.J., Collazo, A., et al. (2012). De novo somatic mutations in components of the PI3K-AKT3-mTOR pathway cause hemimegalencephaly. Nat. Genet. *44*, 941–945.
4. Lim, J.S., Kim, W.I., Kang, H.C., Kim, S.H., Park, A.H., Park, E.K., Cho, Y.W., Kim, S., Kim, H.M., Kim, J.A., et al. (2015). Brain somatic mutations in MTOR cause focal cortical dysplasia type II leading to intractable epilepsy. Nat. Med. *21*, 395–400.
5. Nakashima, M., Saitsu, H., Takei, N., Tohyama, J., Kato, M., Kitaura, H., Shiina, M., Shirozu, H., Masuda, H., Watanabe, K., et al. (2015). Somatic Mutations in the MTOR gene cause focal cortical dysplasia type IIb. Ann. Neurol. *78*, 375–386.
6. Poduri, A., Evrony, G.D., Cai, X., Elhosary, P.C., Beroukhim, R., Lehtinen, M.K., Hills, L.B., Heinzen, E.L., Hill, A., Hill, R.S., et al. (2012). Somatic activation of AKT3 causes hemispheric developmental brain malformations. Neuron *74*, 41–48.
7. Helbig, I., and Lowenstein, D.H. (2013). Genetics of the epilepsies: where are we and where are we going? Curr. Opin. Neurol. *26*, 179–185.
8. Lindhout, D. (2008). Somatic mosaicism as a basic epileptogenic mechanism? Brain *131*, 900–901.
9. Kang, S., Graham, J.M., Jr., Olney, A.H., and Biesecker, L.G. (1997). GLI3 frameshift mutations cause autosomal dominant Pallister-Hall syndrome. Nat. Genet. *15*, 266–268.
10. Wallace, R.H., Freeman, J.L., Shouri, M.R., Izzillo, P.A., Rosenfeld, J.V., Mulley, J.C., Harvey, A.S., and Berkovic, S.F. (2008). Somatic mutations in GLI3 can cause hypothalamic hamartoma and gelastic seizures. Neurology *70*, 653–655.
11. Craig, D.W., Itty, A., Panganiban, C., Szelinger, S., Kruer, M.C., Sekar, A., Reiman, D., Narayanan, V., Stephan, D.A., and Kerrigan, J.F. (2008). Identification of somatic chromosomal abnormalities in hypothalamic hamartoma tissue at the GLI3 locus. Am. J. Hum. Genet. *82*, 366–374.
12. Saitsu, H., Sonoda, M., Higashijima, T., Shirozu, H., Masuda, H., Tohyama, J., Kato, M., Nakashima, M., Tsurusaki, Y., Mizuguchi, T., et al. (2016). Somatic mutations in GLI3 and OFD1 involved in sonic hedgehog signaling cause hypothalamic hamartoma. Ann Clin Transl Neurol Epub, Mar 24th.
13. Rosenfeld, J.V., Harvey, A.S., Wrennall, J., Zacharin, M., and Berkovic, S.F. (2001). Transcallosal resection of hypothalamic hamartomas, with control of seizures, in children with gelastic epilepsy. Neurosurgery *48*, 108–118.
14. EuroEPINOMICS-RES Consortium; Epilepsy Phenome/Genome Project; Epi4K Consortium (2014). De novo mutations in synaptic transmission genes including DNM1 cause epileptic encephalopathies. Am. J. Hum. Genet. *95*, 360–370.
15. Epi4K Consortium; Epilepsy Phenome/Genome Project (2013). De novo mutations in epileptic encephalopathies. Nature *501*, 217–221.
16. Cibulskis, K., Lawrence, M.S., Carter, S.L., Sivachenko, A., Jaffe, D., Sougnez, C., Gabriel, S., Meyerson, M., Lander, E.S., and Getz, G. (2013). Sensitive detection of somatic point mutations in impure and heterogeneous cancer samples. Nat. Biotechnol. *31*, 213–219.
17. Koboldt, D.C., Zhang, Q., Larson, D.E., Shen, D., McLellan, M.D., Lin, L., Miller, C.A., Mardis, E.R., Ding, L., and Wilson, R.K. (2012). VarScan 2: somatic mutation and copy number alteration discovery in cancer by exome sequencing. Genome Res. *22*, 568–576.
18. Kanehisa, M., and Goto, S. (2000). KEGG: kyoto encyclopedia of genes and genomes. Nucleic Acids Res. *28*, 27–30.
19. Kebenko, M., Drenckhan, A., Gros, S.J., Jücker, M., Grabinski, N., Ewald, F., Grottke, A., Schultze, A., Izbicki, J.R., Bokemeyer, C., et al. (2015). ErbB2 signaling activates the Hedgehog pathway via PI3K-Akt in human esophageal adenocarcinoma: identification of novel targets for concerted therapy concepts. Cell. Signal. *27*, 373–381.
20. Clark, V.E., Erson-Omay, E.Z., Serin, A., Yin, J., Cotney, J., Ozduman, K., Avşar, T., Li, J., Murray, P.B., Henegariu, O., et al. (2013). Genomic analysis of non-NF2 meningiomas reveals mutations in TRAF7, KLF4, AKT1, and SMO. Science *339*, 1077–1080.
21. Ulloa, F., and Martí, E. (2010). Wnt won the war: antagonistic role of Wnt over Shh controls dorso-ventral patterning of the vertebrate neural tube. Dev. Dyn. *239*, 69–76.
22. Zou, Y. (2004). Wnt signaling in axon guidance. Trends Neurosci. *27*, 528–532.
23. Dai, P., Akimaru, H., Tanaka, Y., Maekawa, T., Nakafuku, M., and Ishii, S. (1999). Sonic Hedgehog-induced activation of the Gli1 promoter is mediated by GLI3. J. Biol. Chem. *274*, 8143–8152.
24. Shin, S.H., Kogerman, P., Lindström, E., Toftgård, R., and Biesecker, L.G. (1999). GLI3 mutations in human disorders mimic Drosophila cubitus interruptus protein functions and localization. Proc. Natl. Acad. Sci. USA *96*, 2880–2884.
25. Goh, G., Scholl, U.I., Healy, J.M., Choi, M., Prasad, M.L., Nelson-Williams, C., Kunstman, J.W., Korah, R., Suttorp, A.C., Dietrich, D., et al. (2014). Recurrent activating mutation in PRKACA in cortisol-producing adrenal tumors. Nat. Genet. *46*, 613–617.
26. Sato, Y., Maekawa, S., Ishii, R., Sanada, M., Morikawa, T., Shiraishi, Y., Yoshida, K., Nagata, Y., Sato-Otsubo, A., Yoshizato, T., et al. (2014). Recurrent somatic mutations underlie corticotropin-independent Cushing's syndrome. Science *344*, 917–920.
27. Jamuar, S.S., and Walsh, C.A. (2014). Somatic mutations in cerebral cortical malformations. N. Engl. J. Med. *371*, 2038.
28. Scales, S.J., and de Sauvage, F.J. (2009). Mechanisms of Hedgehog pathway activation in cancer and implications for therapy. Trends Pharmacol. Sci. *30*, 303–312.
29. Sheikh, A., Alvi, A.A., Aslam, H.M., and Haseeb, A. (2012). Hedgehog pathway inhibitors - current status and future prospects. Infect. Agent. Cancer *7*, 29.

The American Journal of Human Genetics, Volume *99*

Supplemental Data

Mutations of the Sonic Hedgehog Pathway Underlie Hypothalamic Hamartoma with Gelastic Epilepsy

Michael S. Hildebrand, Nicole G. Griffin, John A. Damiano, Elisa J. Cops, Rosemary Burgess, Ezgi Ozturk, Nigel C. Jones, Richard J. Leventer, Jeremy L. Freeman, A. Simon Harvey, Lynette G. Sadleir, Ingrid E. Scheffer, Heather Major, Benjamin W. Darbro, Andrew S. Allen, David B. Goldstein, John F. Kerrigan, Samuel F. Berkovic, and Erin L. Heinzen

SUPPLEMENTAL INFORMATION

Supplemental Note: ***Additional statistical methods.***
Sequence mutability of genomic regions (genes, pathways) was calculated by summing a trinucleotide based mutation rate estimate [1] (kindly provided by Drs. Shamil Sunyaev and Paz Polak [2]) over each individual's 'callable real estate' [i.e., the regions of the exome, defined by the Consensus Coding Sequence (CCDS) (v14), that had sufficient coverage that a somatic mutation would likely be called if present, or specifically, the part of the exome that was sequenced at least ten times in both leukocyte and hamartoma DNA]. We then investigated the relationship between the presence of somatic mutations in our sample and the trinucleotide-based mutation rate as follows. First, for every base in the consensus coding sequence, we computed the probability of a mutation from the reference to one of the three alternative bases using the trinucleotide-based mutation rate estimate. From this we were able to compute the exome-wide median mutation probability. For each somatic mutation, we calculated the same probability of a mutation occurring at that site based on the trinucleotide mutation rate estimate. If this mutation rate is independent of the presence of a somatic mutation, we would expect that the mutation probabilities we observed would be a random sample from the overall mutation probability distribution and that about half of them would fall above the exome-wide median and half would fall below. However, we observed 43 somatic mutations were below the median and 140 were above, which is highly significant by the sign test (p=2.334e-11). Second, we conditioned on the trinucleotide context in which the somatic mutations occurs, and asked: given the three possible bases that a site could be mutated to, is the trinucleotide-based mutation rate affiliated with the observed somatic mutation more likely to be the highest of the three rates. We found that 64 somatic mutations were affiliated with the highest trinucleotide-based rate, 33 were affiliated with the lowest, and 76 had intermediate values. Again, we find significant enrichment for high mutation rates (sign test, p=0.002152) and conclude that the trinucleotide mutation rate estimates are positively correlated with occurrence of somatic mutations (and/or amplification artifacts). This finding motivated the incorporation of mutatability in our enrichment testing below.

The pathway enrichment analysis was performed by comparing the observed number of candidate variants in a pathway within each individual to that expected based on mutation rate. Specifically, for a given individual, we conditioned on the total number of mutations observed across their exome and computed the difference between the observed number of candidate variants within a gene or pathway to that expected given the proportion of the total mutability found within the pathway. Note that both the mutability of any gene, as well as the exome-wide mutability can vary from individual to individual, since each individual's 'callable real estate' can vary as described above. Also, note that this observed versus expected contrast is calculated within each individual, and therefore, explicitly accounts for differences in overall rates due to amplification. Individual departures from expectation are standardized by a variance estimate and then summed to give the observed test statistic. We estimate the null distribution of the test statistic by randomly distributing (100,000 times) the total number of mutations in each individual in accordance with the proportion of the total mutability found within the pathway and computing the statistic as described above. In calculating a p-value, we compute the proportion of simulated statistics that are as extreme or more extreme than that computed from the observed somatic mutatons. To account for the large number of hypotheses tested in each analysis we computed adjusted p-values using the resampling procedure of Ge et al. (2003) [3]. Gene-level enrichment analyses, comparing the observed number of candidate variants within each individual to that expected based on the mutation rate, were performed identically to the pathway enrichment analysis with the analysis unit being an individual gene rather than a list of genes comprising a pathway. To correct for the ~18,000 protein-coding genes defined in the CCDS, we used the more stringent Bonferroni correction.

The simulation analysis to assess the significance of gene enrichment in the Shh and salivary secretion pathways involved randomly shuffling CNVs or LOH events throughout the genome and assessing how often Shh and salivary secretion pathways are impacted by these events. Specifically, for each simulated dataset, we randomly placed, throughout the genome, CNVs or LOH events that were the same sizes as the CNVs or LOH events found by CMA. We then counted the number of genes in the Shh or salivary pathways that overlapped with simulated CNV or LOH events for each simulated dataset. The proportion

of simulated datasets for which the number of genes hit by the simulated lesions in these pathways greater than or equal to that found by CMA defined an empirical p-value for this assessment.

SUPPLEMENTAL FIGURES

Figure S1: Copy number mutations detected by CMA

For the Affymetrix CytoScan HD microarray experiments, processing of samples was performed by end point PCR amplification using DNA Taq polymerase (Clontech, Inc.; Mountain View, CA). The labeled patient DNA was hybridised to a human whole genome array containing 1.9 million non-polymorphic markers, as well as 750,000 SNP probes (Affymetrix; Santa Clara, CA), according to the manufacturer's instructions. Post-hybridisation procedures were performed according to the manufacturer's instructions. The ChAS (Chromosome Analysis Software) tool (version 1.1.2; Affymetrix) was used for feature extraction, calculation of log2 ratio values, and calculation of several quality control metrics according to the manufacturer's instructions. CNV calling and data interpretation were performed with the .CEL files using the Nexus Copy Number software tool (version 7.5, BioDiscovery; El Segundo, CA) and SNP-FASST2 and SNP-RANK algorithms supplied with the Nexus software suite. A minimum size threshold of 200-kb was used. **A.** Chromosomal microarray of hamartoma tissue in HH patient hht25063 showing copy number gain of chromosome 7p and copy number loss of chromosome 7q. **B.** Chromosomal microarray of blood in HH patient hht25063 showing normal copy number across chromosome 7.

A.

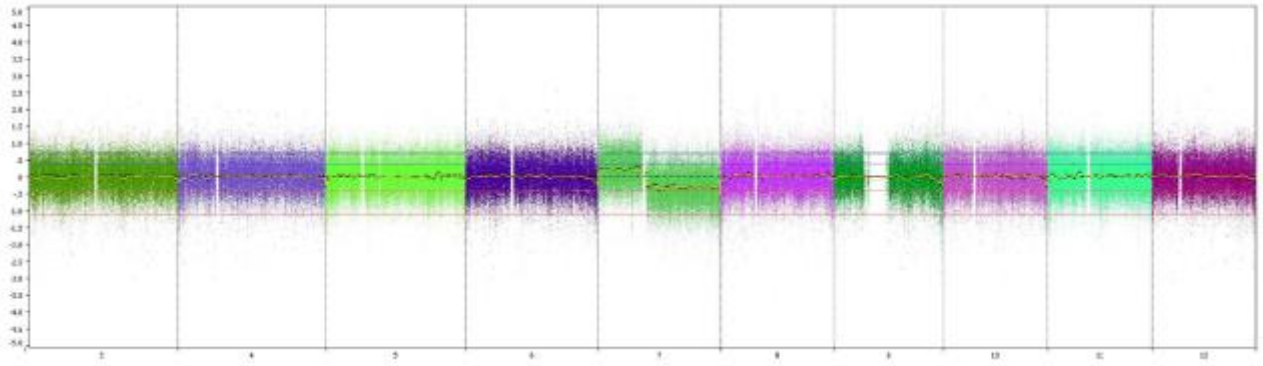

B.

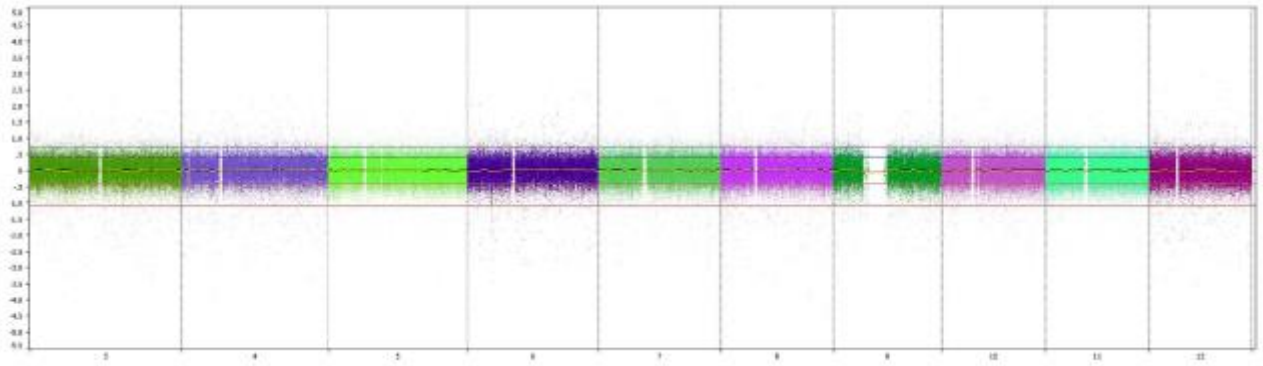

Figure S2: Copy number mutations detected by WES

Somatic LOH variants were filtered by requiring that there be at least five consecutive exonic LOH calls that spanned at least 1-kb (including noncoding sequence) with at least 10-fold sequencing coverage. To estimate the boundaries of the LOH event we plotted all germline variant calls with at least 25-fold coverage in hamartoma and leukocytes with a variant allele frequency between 40% and 60% and all LOH calls meeting the above criteria. **A.** A large region of homozygosity (ROH) on chromosome 7q indicates a loss of heterozygosity (LOH) in HH patient hht1198 that includes the *SMO* and *SHH* genes. **B.** ROH on chromosome 16p indicates a large somatic region of LOH in HH patient hht735 that includes the *CREBBP* gene. In **A** and **B** black dots indicate germline variant calls, and red dots indicate LOH variant calls.

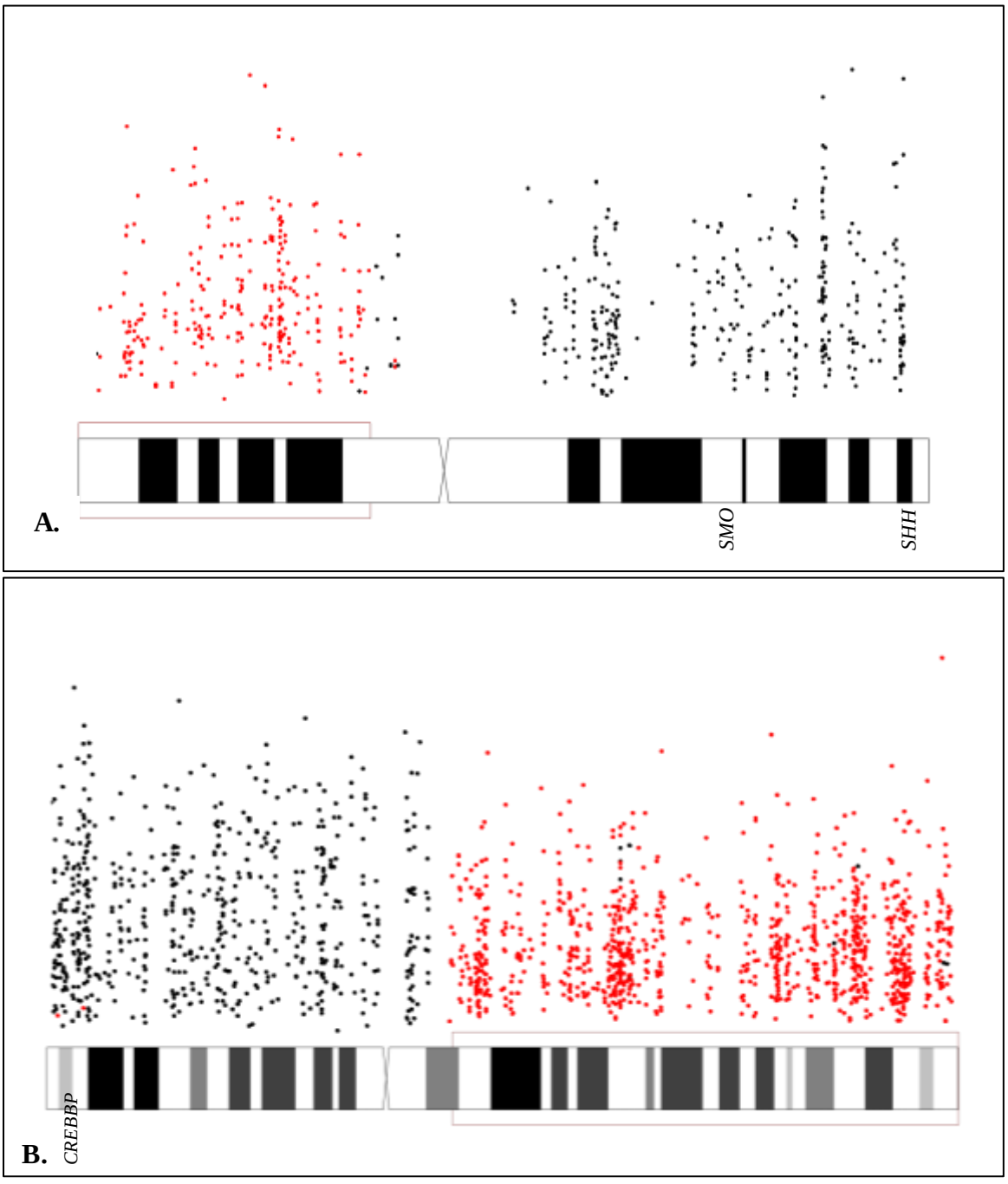

SUPPLEMENTAL TABLES

Table S1: Summary of clinical data from 38 patients

Patient Number	Shh Gene (KEGG)	Gender	Seizure types	Seizure frequency	Refractory (Y/N)	Age of onset	Age at surgery	IQ<70 (Y/N)	Precocious puberty	HH type [4]	Volume (cm^3)
hht25057	*CREBBP*[a]	M	Multi	11-20/day	Y	1 month	16 years	Y	Y	2	1.26
hht25063	*GLI3, SHH, SMO, WNT16, WNT2*	F	Multi	6-10/day	Y	1 month	2 years	N	N	2	0.74
hht25085	*PRKACA*	F	Multi	1-5/day	Y	5 years	17 years	N	N	3	1.06
hht25086	*PRKACA*	M	Gelastic	11-20/day	Y	1 month	3 years	Y	N	3	4.14
hht25077	*GLI3*	F	Multi	1-5/day	Y	3 months	10 years	N	N	2	0.24
hht25094	*WNT11*	F	Gelastic	1-5/day	Y	4 years	8 years	Y	Y	2	0.07
hht209	*GLI3*	M	Multi	1-5/day	Y	Birth	10 years	Y	N	2	0.33
hht26139	*GLI3*	M	Multi	1-5/day	Y	Birth	4 years	Y	N	2	0.58
hht238a	*PRKACA*	F	Multi	1-5/day	Y	Birth	8 years	N	Y	2	1.94
hht1198c	*SHH, SMO, WNT16, WNT2*	F	Multi	11-20/day	Y	Birth	13 years	Y	Y	3	3.39
hht735	*CREBBP*[a]	M	Multi	1-5/day	Y	Birth	9 years	Y	Y	3	14.21
hht953	*BMP4*	M	Multi	6-10/day	Y	Birth	23 years	N	N	2	1.21
hht880	*GLI2, IHH, LRP2, STK36, WNT10A, WNT6*	M	Multi	6-10/day	Y	2 years	9 years	Y	N	2	0.69
hh31536	*GLI3*	M	Gelastic	6-10/day	Y	Birth	22 months	N	N	2	0.13
hht25056		M	Multi	6-10/day	Y	3 years	12 years	Y	N	3	0.42
hht25059		F	Gelastic	11-20/day	Y	1 month	5 years	N	N	3	2.91
hht25050		M	Multi	1-5/day	Y	7 years	31 years	Y	N	2	0.13
hht25092		M	Multi	1-5/day	Y	7 years	15 years	Y	Y	1	0.04
hht25186		F	Multi	1-5/day	Y	1 month	8 years	N	N	2	0.66
hht25093g		M	Multi	6-10/day	Y	1 month	18 years	Y	Y	2	1.91
hht25079		M	Multi	1-5/day	Y	9 months	29 years	Y	N	4	4.51
hht25097		M	Multi	1-5/day	Y	6 months	13 years	Y	N	2	0.91
hht25098		M	Multi	1-5/day	Y	1 month	19 years	Y	N	2	1.10
hht25080		M	Multi	1-5/day	Y	2 years	22 years	N	Y	2	0.19
hht25099		M	Multi	1-5/day	Y	8 months	9 years	Y	N	2	0.57
hht25082		M	Multi	1-5/day	Y	1 month	14 months	Y	N	2	0.15

hht25132h		M	Multi	6-10/day	Y	3 months	11 years	N	N	2	0.20
hht322b		F	Multi	1-5/day	Y	3 months	4 years	N	N	2	0.56
hht786		F	Multi	6-10/day	Y	Birth	8 years	N	Y	2	1.12
hht929		M	Multi	6-10/day	Y	Birth	5 years	Y	N	2	2.14
hht1276d		M	Multi	1-5/day	Y	12 months	10 years	Y	N	2	1.43
hht20138		F	Multi	11-20/day	Y	9 months	13 years	N	Y	3	1.04
hht25052		M	Multi	11-20/day	Y	1 month	2 years	Y	N	2	0.34
hht25054		M	Multi	1-5/day	Y	1 month	13 years	Y	Y	4	8.23
hht25060		M	Multi	1-5/day	Y	1 month	24 years	Y	Y	2	1.29
hht25064		M	Gelastic	2/week	Y	1 month	11 years	N	Y	2	1.34
hht25066		M	Gelastic	11-20/day	Y	1 month	2 years	Y	Y	3	2.05
hht25072		M	Multi	11-20/day	Y	2 years	4 years	Y	Y	2	2.05

[a]***Transcriptional regulator of the Shh pathway;*** **F: female; M: male; Multi: multiple seizure types; N: no; Y: yes**

Table S2: Coverage and mutational burden summary of somatic variants from whole exome sequencing of tumor and leucocyte-derived DNA in 15 HH patients. sSNV= somatic single nucleotide variant; sindel= somatic indel.

	Amplified	Brain tissue coverage	Blood coverage	% of Shh genes sequenced at least 10-fold in paired DNA samples	All sSNVs	Candidate sSNVs	All sindels	Candidate sindels
hht238a	no	122.73	225.92	87.9%	193	2	221	1
hht322b	no	67.07	184.13	86.6%	269	3	200	0
hht1198c	no	92.16	82.01	85.9%	136	2	167	0
hht1276d	no	103.48	202.19	88.2%	154	2	229	0
hht25093g	no	62.54	101.87	84.8%	164	4	162	0
hht25132h	no	92.01	107.06	85.1%	135	7	138	0
hht209	yes	134.33	148.97	83.2%	681	77	577	13
hht735	yes	146.43	108.65	77.6%	1755	9	163	3
hht786	yes	135.49	107.78	79.8%	254	5	163	3
hht929	yes	78.84	173.07	69.5%	180	6	762	26
hht25080	yes	150.64	124.72	83.4%	242	4	198	4
hht25082	yes	140.54	127.65	79.1%	238	5	199	3
hht25086	yes	178.71	95.72	68.8%	398	9	174	2
hht25099	yes	180.15	36.7	50.2%	665	33	115	0
hht26139	yes	120.19	153.16	74.7%	148	5	347	0
Mean		**120**	**132**	**79.0%**	**374**	**12**	**254**	**4**
Standard Deviation		**37**	**50**	**10.0%**	**421**	**20**	**180**	**7**

Table S3: Candidate somatic variants called from WES and TRS of paired harmatoma-leukocyte DNA samples from individuals with HH

See excel sheet attached.

SUPPLEMENTAL REFERENCES

1. Kryukov, G.V., Pennacchio, L.A., and Sunyaev, S.R. (2007). Most rare missense alleles are deleterious in humans: implications for complex disease and association studies. Am J Hum Genet 80, 727-739.
2. Francioli, L.C., Polak, P.P., Koren, A., Menelaou, A., Chun, S., Renkens, I., van Duijn, C.M., Swertz, M., Wijmenga, C., van Ommen, G., et al. (2015). Genome-wide patterns and properties of de novo mutations in humans. Nat Genet 47, 822-826.
3. Ge, Y., Dudroit, S., and Speed, T.P. (2003). Resampling-based multiple testing for microarray data hypothesis. Test 12, 1-77.

SUPPLEMENTAL ACKNOWLEDGEMENTS

We would like to acknowledge the following individuals or groups for the contribution of control samples: D. Daskalakis; R Buckley; M. Hauser; J. Hoover-Fong, N. L. Sobreira and D. Valle; A. Poduri; T. Young and K. Whisenhunt; Z. Farfel, D. Lancet, and E. Pras; R. Gbadegesin and M. Winn; K. Schmader, S. McDonald, H. K. White and M. Yanamadala; R. Brown; S. H. Appel; E. Simpson; S. Halton, L. Lay; A. Holden; E. Behr; C. Moylan; A. M. Diehl and M. Abdelmalek; S. Palmer; G. Cavalleri; N. Delanty; G. Nestadt; D. Marchuk; V. Shashi; M. Carrington; R. Bedlack,; M. Harms; T. Miller; A. Pestronk; R. Bedlack; R. Brown; N. Shneider; S. Gibson; J. Ravits; A. Gilter; J. Glass; F. Baas; E. Simpson; and G. Rouleau; The ALS Sequencing Consortium; The Murdock Study Community Registry and Biorepository; the Carol Woods and Crosdaile Retirement Communities; Washington University Neuromuscular Genetics Project; the Utah Foundation for Biomedical Research; and DUHS (Duke University Health System) Nonalcoholic Fatty Liver Disease Research Database and Specimen Repository. The collection of control samples and data was funded in part by: Biogen Idec.; Gilead Sciences, Inc.; New York-Presbyterian Hospital; The Columbia University College of Physicians and Surgeons; The Columbia University Medical Center; The Duke Chancellor's Discovery Program Research Fund 2014; Bill and Melinda Gates Foundation; The Stanley Institute for Cognitive Genomics at Cold Spring Harbor Laboratory; B57 SAIC-Fredrick Inc M11-074; The Ellison Medical Foundation New Scholar award AG-NS-0441-08; National Institute of Mental Health (K01MH098126, R01MH099216, R01MH097993); National Institute of Allergy and Infectious Diseases (1R56AI098588-01A1); National Human Genome Research Institute (U01HG007672); National Institute of Neurological Disorders and Stroke (U01-NS077303, U01-NS053998); and National Institute of Allergy and Infectious Diseases Center (U19-AI067854, UM1-AI100645).